Changes in quantitative ultrasound parameters during HIFU application

Goutam Ghoshal, Jeremy P. Kemmerer, and Michael L. Oelze

Citation: AIP Conf. Proc. **1481**, 106 (2012); doi: 10.1063/1.4757319
View online: http://dx.doi.org/10.1063/1.4757319
View Table of Contents: http://proceedings.aip.org/dbt/dbt.jsp?KEY=APCPCS&Volume=1481&Issue=1
Published by the American Institute of Physics.

Changes in Quantitative Ultrasound Parameters during HIFU Application

Goutam Ghoshal, Jeremy P. Kemmerer, and Michael L. Oelze

Bioacoustics Research Laboratory, Department of Electrical and Computer Engineering, University of Illinois at Urbana-Champaign, 405 N. Mathews, Urbana, IL 61801 USA

Abstract. Quantitative ultrasound (QUS) is a novel imaging technique that is hypothesized to be capable of monitoring of High Intensity Focused Ultrasound (HIFU) treatment by quantifying tissue changes during exposure. Experiments were conducted on fresh liver samples from rats and lesions were formed using a HIFU system (1-MHz, f/1.2). A wire thermocouple was inserted into the sample to monitor temperature elevation. Backscattered time domain waveforms were recorded using a clinical imaging system (Ultrasonix, L14-5 linear array) during the HIFU application and backscatter coefficients were estimated using a reference phantom technique. Two parameters were estimated from the backscatter coefficient (effective scatterer diameter (ESD) and effective acoustic concentration (EAC)) and two parameters were estimated from the envelope statistics (k parameter and μ parameter) of the backscattered echoes. At the end of the exposure the ESD, EAC and k parameters changed in the treated region by 20%, 50% and 15% respectively, compared to the untreated region. Furthermore, changes in QUS parameters followed the shape of the temperature profile recorded by the thermocouple. These results suggest that QUS techniques could be used for noninvasive thermometry of HIFU.

Keywords: HIFU, quantitative ultrasound, ultrasonic scattering, envelope statistics
PACS: 43.80.Ev, 43.80.Sh, 43.80.Vj

INTRODUCTION

High intensity focused ultrasound (HIFU) is a promising technique for clinical therapies involving noninvasive thermal ablation or hyperthermia. HIFU allows the targeting of small regions for thermal ablation or hyperthermia treatment and has been successfully demonstrated in animal models of cancer and in limited clinical studies and treatments. For example, currently HIFU therapy has been approved in the U.S. for the treatment of uterine fibroids [1, 2]. To promote further clinical use of HIFU therapy, a robust imaging and monitoring system is essential [3]. Ultrasound, X-ray CT, and MRI have been examined as tools to monitor the temperature rise in tissue treated with HIFU and to guide exposures. Currently MRI is considered the most accurate and robust method to monitor and quantify temperature elevations in tissues treated with HIFU noninvasively and in the presence of tissue motion. However, MRI is an expensive imaging modality and requires specialized HIFU equipment in order not to interfere with the MRI system.

Ultrasound is an attractive imaging modality to guide and monitor HIFU treatment because it is non-ionizing, inexpensive, portable, real time, and convenient. Because of its attractiveness, several ultrasonic techniques have been investigated for

11th International Symposium on Therapeutic Ultrasound
AIP Conf. Proc. 1481, 106-111 (2012); doi: 10.1063/1.4757319

monitoring, quantifying, and mapping the temperature rise induced in tissues by HIFU treatment. These techniques include quantifying changes in speed of sound, attenuation, and elastic properties [4]. However, these techniques are susceptible to tissue motion resulting in inaccurate temperature maps and elastic properties.

Quantitative ultrasound (QUS) techniques have been successfully used to characterize tissue microstructure [5]. Previous experiments with biological phantoms and fresh liver samples in a saline bath indicated that QUS techniques could predict temperature elevations in tissues [6, 7]. Therefore, QUS may also be used to monitor temperature elevations induced in tissues due to HIFU treatment.

To test the ability of QUS to monitor temperature elevations in tissues during HIFU application, experiments with fresh rat liver samples were conducted. A single-element focused transducer was used for HIFU applications and a linear array transducer was used to acquire radio-frequency (rf) signals during the HIFU application. The temperature profile during the HIFU was obtained from a thermocouple inserted near the focus of the HIFU transducer. The characteristics of the various QUS parameters and the temperature profile from the thermocouple were compared to quantify the potential of QUS to monitor temperature elevations in tissues.

EXPERIMENTAL METHODS

Liver Samples

Fresh liver samples were extracted from Sprague Dawley rats (Harlan Laboratories, Inc, Indianapolis, IN). Each liver sample was immersed in a saline bath made from degassed water immediately after the extraction from the body and later embedded in a 2.5% agar base phantom. The phantom was constructed by mixing 2.5% agar with degassed water and heated to 80°C. Once the solution decreased to a temperature of 48°C, the solution was poured into a six-well plate and partially filled. Then a single lobe of the liver sample was dropped into the well and the well was filled to the rim with agar solution. The plate was refrigerated for 30 minutes at 4°C, and then maintained at room temperature for an additional fifteen minutes before the ultrasonic experiments were conducted. The liver samples were embedded in the agar phantom in order to securely hold the samples. No visible whitening of the livers occurred after embedding them in the warm agar.

Ultrasonic Methods

Agar phantoms containing a single lobe of rat liver were exposed to a single-element 1-MHz (f/1.1) transducer powered by an A150 55 dB power amplifier (ENI) and excited by an arbitrary waveform generator (HP 33120a, Agilent Technologies, Santa Clara, CA). The exposure was monitored using a SonixRP clinical ultrasound system (Ultrasonix, Richmond, BC, Canada) with an L14-5/38 probe sampled at 40 MHz. The probe had a nominal center frequency of 6 MHz. The array probe and single-element HIFU transducer were aligned by creating a single lesion in an agar phantom with the HIFU system, and aligning the array transducer to this lesion visible

in the B-mode display of the clinical imaging system. The array system and HIFU transducer were thus aligned and remained fixed throughout the experiment, and the location of this lesion was marked on the SonixRP B-mode display and used for targeting in the HIFU liver experiment. The experimental setup, including transducer and sample orientation, is shown in Figure 1. The temperature near the focus of the single-element transducer was monitored by a wire thermocouple (HSTC-TT-T-24S-36-SMPW-CC, Omega Engineering, Inc., Stamford, Connecticut) inserted into the liver sample. The thermocouple was connected to a temperature reader (NI USB-TC01, National Instruments Corporation, Austin, Texas), which was connected to a computer to record temperature every one second. The saline bath was maintained at 37°C using an automatic temperature controller throughout the ultrasonic experiment. In an experiment, the sample was moved using a computer-controlled micropositioning system (Daedal, Inc., Harrisburg, PA).

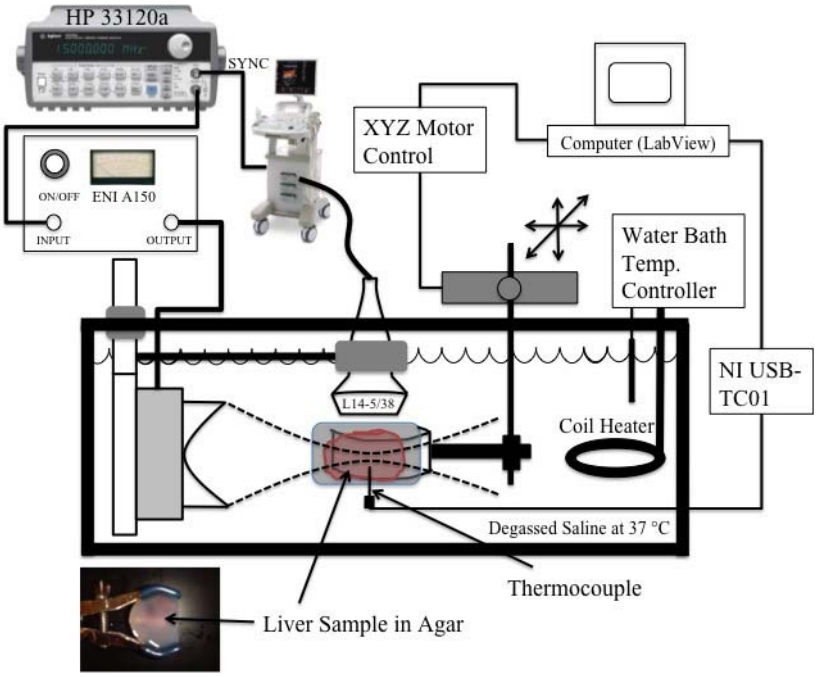

FIGURE 1. Experimental setup.

The liver samples were exposed for 15 seconds. Exposure intensities varied between 1500 and 2500 W/cm^2 with 50% duty cycle, as measured in degassed water using a needle hydrophone (Precision Acoustics, Dorchester, UK). Data was collected using the clinical system during the exposure by synchronizing the capture of the RF data with periods between HIFU exposure tone-bursts.

B-mode images of the scanned areas were constructed. Regions of interest (ROIs) in the B-mode images were examined for the spectral content of the backscattered rf echoes. Square shaped data blocks of size 10λ by 10λ (λ is the wavelength) were constructed with 80% overlap between adjacent data blocks both in the vertical and horizontal directions. The backscatter coefficient (BSC) was estimated for each data block from the backscattered rf signals using the reference phantom technique [8]. The reference scan was obtained from a well-characterized reference phantom.

Estimates of the ESD were obtained by using a spherical Gaussian scattering model. In the frequency domain, the normalized, theoretical power spectrum is given by [9, 10]

$$W(f) = \frac{185 L q^2 a_{\text{eff}}^6 \rho z_{\text{var}}^2 f^4}{1 + 2.66\left(f q a_{\text{eff}}\right)^2} \exp\left[-12.159 f^2 a_{\text{eff}}^2\right], \quad (1)$$

where L is the gate length (mm), q is the ratio of aperture radius to distance from the region of interest, f is the frequency (MHz) and a_{eff} is the effective scatterer radius. The quantity, ρz_{var}^2, is termed the effective acoustic concentration (EAC) and is the product of the number of scattering particles per unit volume (mm^3), ρ, and the square of the fractional change in the impedance between the scattering particles and the surrounding medium, $z_{\text{var}} = \left(Z - Z_0\right)/Z_0$, where Z and Z_0 are the acoustic impedance of the scatterers and the surrounding medium respectively. The ESD and EAC were determined by comparing the measured normalized power spectrum from each data block to the theoretical power spectrum from Eq. (1).

The organization of the underlying tissue microstructure was also characterized versus temperature through the envelope statistics. The homodyned K distribution was used to model the amplitude of the envelope from data blocks in the liver sample [11, 12]. The homodyned K distribution yields two parameters: the k parameter quantifies the ratio of coherent to incoherent backscattered signal and the μ parameter quantifies the number of scatterers per resolution cell. A method based on level curves was used to estimate homodyned K parameters [13]. Estimates of the k parameter and the μ parameter were obtained from backscattered envelope signals corresponding to data blocks in the liver samples.

EXPERIMENTAL RESULTS

B-mode images of the liver samples at different time points of HIFU application are shown in Figs. 2(a), (d) and (g) and the corresponding parametric image enhanced by ΔEAC are shown in Figs. 2(b), (e) and (h). The temperature profiles recorded by the thermocouple are shown as the blue curves in Figs. 2(c), (f) and (i). The red circles indicate the time points corresponding to the displayed B-mode and parametric images. The changes in ΔEAC (%) are shown in Figs. 2(c), (f) and (i) in green color. The percentage changes in EAC versus time were estimated using $\Delta ESD\%(10\ \text{sec}) = 100 \times \left[ESD(10\ \text{sec}) - ESD(0\ \text{sec})\right]/ESD(0\ \text{sec})$. An attenuation correction of 0.7 dB/cm/MHz was used to obtain the BSCs at different time points of HIFU application. It is expected that the lesion created by the HIFU application will have spatially varying attenuation, but the results shown do not account for attenuation changes in the lesion.

Overall three liver samples were used for the experiments to estimate the changes

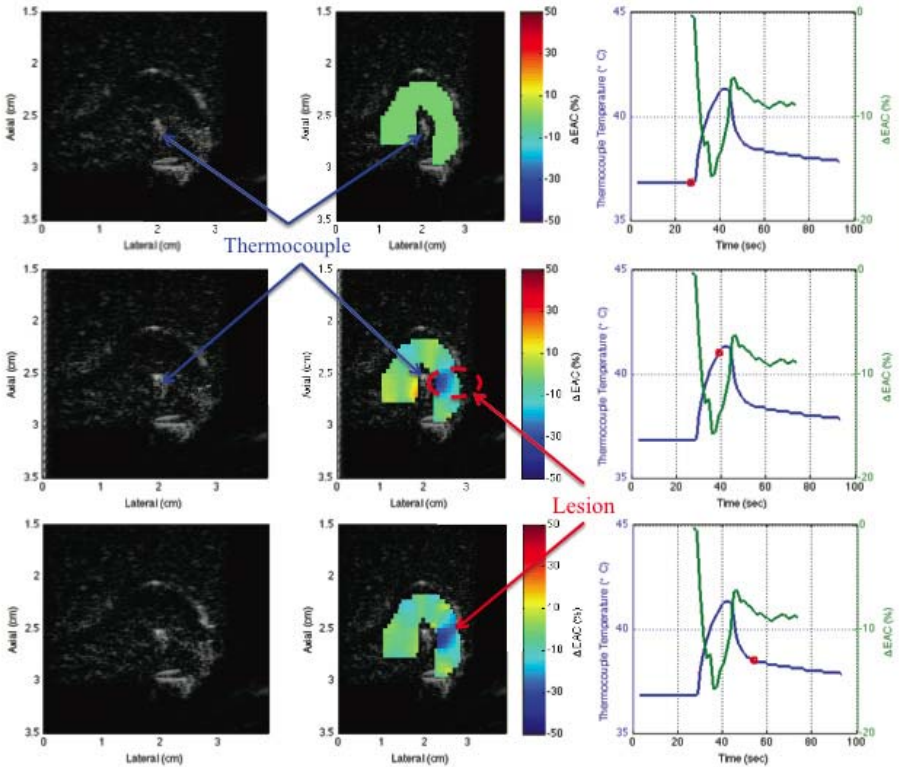

FIGURE 2. Parametric images at different times during HIFU application.

in various QUS parameters with HIFU application in fresh liver samples embedded in agar phantom. An example of the changes observed in all of the QUS parameters are shown in Fig. 3. The ESD was observed to increase with application of HIFU, but it continued to increase even after HIFU was turned off. The EAC was observed to decrease as the temperature increased and then increased once again as the HIFU was turned off and the temperature decreased. Because the EAC did not appear to return to its initial value at the HIFU focus, it is possible that a permanent change in the tissue properties occurred. Therefore, it is possible that the EAC could be used to assess lesion formation. Significant changes in EAC were observed in the HIFU treated regions compared to the untreated region (i.e., EAC increased by 50%). The maximum increase of the k parameter during the exposure was 25% in the HIFU treated region compared to the untreated region. No significant trends in the μ parameter were observed in all the three samples for treated versus untreated during the HIFU exposure. All the three samples showed similar characteristics for changes in EAC and k parameter with application of heat. One out of the three samples showed less than 2% change in ESD with application of HIFU.

CONCLUSION

Lesions were formed using HIFU in fresh rat liver samples embedded in agar and the QUS imaging technique was used to monitor temperature elevations due to HIFU. From the results it was observed that some QUS parameters were more sensitive to HIFU interactions with the tissues than others. Interestingly, the changes in EAC and k

tracked the temperature profile recorded by the thermocouple. The results suggest that QUS has the potential to be used for noninvasive monitoring of temperature elevation due to HIFU application.

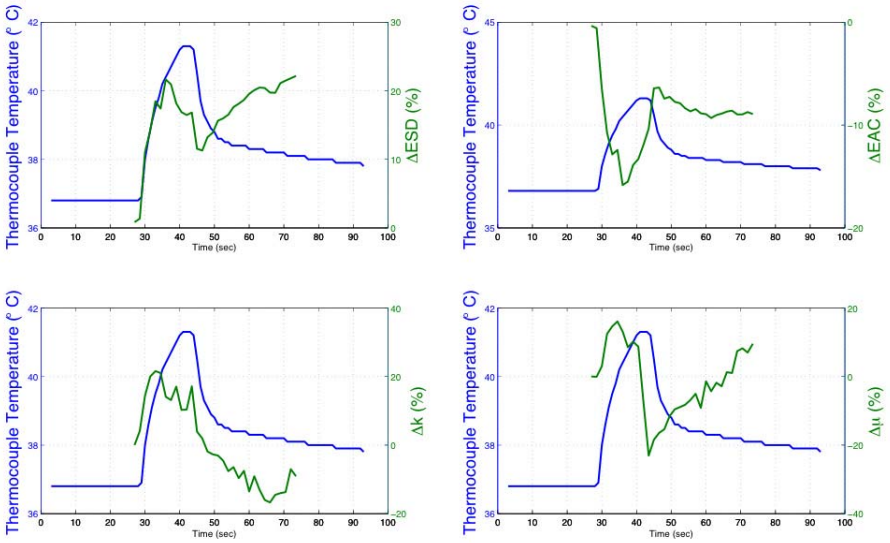

FIGURE 3. Experimental results in terms of changes in (a) ΔESD, (b) ΔEAC, (c) Δk and (d) Δμ versus time. The green curve shows the temperature profile recorded by the thermocouple.

ACKNOWLEDGMENTS

The authors would like to acknowledge the technical contributions of Dr. Rita J. Miller. The work was supported by NIH Grant R01-EB008992.

REFERENCES

1. E. A. Stewart,W. M. Gedroyc, C. M. Tempany, B. J. Quade, Y. Inbar, T. Ehrenstein, A. Shushan, J. T. Hindley, R. D. Goldin, M. David, M. Sklair, and J. Rabinovici, Am. J. Obstet. Gynecol. 189, 48–54 (2003).
2. C. M. Tempany, E. A. Stewart, N. McDonald, B. J. Quade, F. A. Jolesz, and K. Hynynen, Radiology 226, 897–905 (2003).
3. G. T. Clement, Ultrasonics 42, 1087–1093 (2004).
4. J. C. Bamber, and C. R. Hill, Ultrasound Med. Biol. 5, 149–157 (1979).
5. M. L. Oelze, J. F. Zachary, and W. D. O'Brien, Jr., J. Ultrasound Med. 21 (2002).
6. G. Ghoshal, and M. L. Oelze, Proceedings of the 2009 IEEE Ultrasonics Symposium pp. 1780–1783 (2009).
7. G. Ghoshal, and M. L. Oelze, J. Accoust. Soc. Am. (under review) (2011).
8. L. X. Yao, J. A. Zagzebski, and E. L. Madsen, Ultrasonic Imag. 12, 58–70 (1990).
9. F. L. Lizzi, M. Astor, T. Liu, C. Deng, D. J. Coleman, and R. H. Silverman, Int. J. Imaging Syst. Technol. 8, 3–10 (1997).
10. M. Oelze, J. F. Zachary, and W. D. O'Brien, Jr., J. Acoust. Soc. Am. 112, 1202–1211 (2002).
11. V. Dutt, and G. F. Greenleaf, Ultrasonic Imag. 16, 265–287 (1994).
12. M. L. Oelze, W. D. O'Brien, Jr., and J. F. Zachary, Proc. of the 2007 IEEE Ultrasonic Symposium pp. 981–984 (2007).
13. D. P. Hruska, and M. L. Oelze, IEEE Trans. Ultrason. Ferroelectr. Freq. Control 56, 2471–2481 (2009).